



INTENSIFICATION OF THE HEAT TRANSFER THROUGH CORRUGATED WALL

*Donka STOEVA¹

¹University of Food Tehnologies, MAFI Department,
26 Maritsa Blvd; 4000 Plovdiv; BULGARIA

bodurova@gmail.com

*Corresponding author

Received February 17th 2014, accepted March 14th 2014

Abstract: The corrugation of the smooth steel tubes increases the heating surface per length unit. The advantages compared to smooth pipe bodies are the lower relative mass at same thermal power and the smaller volume. The aim of the present research is to trace the temperature alteration near to a specially corrugated wall with baffles. The baffles have variable step towards the flow direction at two different heights. We observe developed turbulent air flow at temperature 353K (80°C) through a corrugated tube with inside diameter $d=0.08\text{m}$ and length 0.2m. The tube wall is heated to 453K (180°C). The heat transfer between the tube and the flowing fluid has been modulated at two different corrugation grades of the tube – X_1 and X_2 – equation (9) and with four different Reynolds numbers.

Key words: CFD, boundary layer, surface baffles, turbulization, circulation zone.

1. Intorduction

The intensity of the heat transfer can be influenced by alteration of the geometric dimensions of the channel, alteration of the velocity of the heat carrier and the form of the heat transfer surface, which defines the temperature field [1, 2, 3].

One of the ways for intensification of the heat flows is by increasing the velocity of the heat carrier or by corrugating the surfaces.

When flowing onto hard wall there is a boundary layer forming. It is the main thermal resistant. The thicker the boundary layer is, the lower the heat transfer is [4, 5, 6].

The decreasing of the boundary layer thickness and the increasing of the transfer coefficients

For moment and heat is the essence of the heat transfer intensification.

Most profitable hydrodynamic regime regarding the heat transfer is the transitional and turbulent regime in the boundary layer. This can be achieved by artificial turbulization of the flow in the boundary layer or destroying of the boundary layer near the wall. This enforces the application of artificial methods for intensification of the heat transfer.

The methods for intensification of heat transfer are divided in two groups: passive and active.

Passive methods are the ones that do not need direct use of outer energy source. Active are those, who use outer source. There are two methods used for intensification of the heat transfer: increase of the heat flow, regardless of the costs and increase of the heat flow at defined power of the heat carrier [1, 2, 3, 4]. The most frequently used passive method is intensification through surface baffles,

such as rough surfaces and equally distributed roughness [5, 6].

The configuration of the baffles is chosen in such a way, so that it destroys the viscosity sub-layer and increases the turbulence near the wall [7, 9, 10].

One of the most important conditions for choosing of method is the hydrodynamic structure of the flow in which we need alteration in the temperature field distribution. Knowing this structure, we can reduce the areas in which the increase of the intensification of the turbulent pulsations will make greatest influence on the heat transfer intensification [1, 7, 8, 9]. The analysis and the visualization of the flow in such tubes are of great importance

because they have wide application in the heating equipment and many other spheres. The aim of the present research is to trace the temperature alteration near to a specially corrugated wall with baffles. The baffles have variable step towards the flow direction at two different heights.

2. Materials and Methods

The model researches are carried out at four different Reynolds numbers (Re). We have used the equation for fluid movement for turbulent regime (equation 1) and we have added two equations for kinetic energy (equation 2)– k and kinetic energy dissipation ε (equation 3)

$$U_i \frac{\partial k}{\partial x_i} = v_t \frac{\partial U_i}{\partial x_j} \left(\frac{\partial U_i}{\partial x_j} + \frac{\partial U_j}{\partial x_i} \right) + \frac{\partial}{\partial x_i} \left[\left(v + \frac{v_t}{\sigma_k} \right) \frac{\partial k}{\partial x_i} \right] - \bar{\varepsilon} - 2v \left(\frac{\partial \sqrt{k}}{\partial x_j} \right)^2 \quad (1)$$

$$v_t = C_\mu \frac{k^2}{\varepsilon} \quad (2)$$

$$U_i \frac{\partial \varepsilon}{\partial x_i} = \frac{\partial}{\partial x_i} \left[\left(v + \frac{v_t}{\sigma_\varepsilon} \right) \frac{\partial \varepsilon}{\partial x_i} \right] + C_{\varepsilon 1} \frac{\varepsilon}{k} v_t \left(\frac{\partial U_i}{\partial x_j} + \frac{\partial U_j}{\partial x_i} \right) \frac{\partial U_i}{\partial x_j} - C_{\varepsilon 2} \frac{\varepsilon^2}{k} \quad (3)$$

The constants are:

$$C_{\varepsilon 1} = 1.44; \quad C_{\varepsilon 2} = \frac{1.92}{(1 + 0.9A^{1/2}A_2)} = 1.92 \quad (4)$$

For solving the heat transfer system of equations we add the equation for energy of the following type:

$$\frac{\partial}{\partial t} (\rho E) + \nabla \cdot (\bar{v} (\rho E + p)) = \nabla \cdot (k_{eff} \nabla T - \sum_j h_j \bar{J}_j + (\bar{\tau}_{eff} \bar{v})) + S_h \quad (5)$$

Where k_{eff} is the **effective conductivity**, k_t is the **turbulent conductivity** defined by the used turbulent model, and \bar{J}_j is a diffusion of the flow type j . The first three nominals at the right side of the equation present the energy transfer through conductivity, the specific diffusion

and the viscous dissipation. S_h includes heat from chemical reactions and others, if such are defined.

$$E = h - \frac{p}{\rho} + \frac{v^2}{2} \quad (6)$$

where the enthalpy h for an incompressive fluids is calculated by equation (7) :

$$h = \sum_j Y_j h_j + \frac{p}{\rho} \quad (7)$$

In the above equations Y_j is the mass fraction of the type j .

$$h_j = \int_{T_{ref}}^T C_{p,j} dT \quad (8)$$

where $T_{ref} = 298.15K$

For the two-dimension case the mesh contains 16500 cells, 33350 faces and 16581 knots as a preliminary test for independence of the solution from the mesh thickness has been performed [3, 4, 9, 10].

We observe developed turbulent air flow at temperature 353K (80°C) through a corrugated tube with inside diameter $d=0.08$ m and length 0,2 m. The tube wall is heated to 453K (180° C). The heat transfer between the tube and the flowing fluid has been modulated at two different corrugation grades of the tube – X_1 and X_2 – equation (9) and with four different Reynolds numbers (we achieve that by setting four different initial velocities at the boundary conditions – equation (10)). The graphic relations are shown for central section in the geometric body and for the outgoing section.

$$X_1 = \frac{h_1}{D} = \frac{0.002}{0.08} = 0.025; \quad X_2 = \frac{h_2}{D} = \frac{0.004}{0.08} = 0.05 \quad (9)$$

$$Re_1 = \frac{V_1 \cdot D}{\nu_{e-x}} = \frac{0.75 \times 0.08}{1.7894 \times 10^{-5}} = 3353.1 \quad Re_2 = \frac{V_2 \cdot D}{\nu_{e-x}} = \frac{1 \times 0.08}{1.7894 \times 10^{-5}} = 4470.8$$

$$Re_3 = \frac{V_3 \cdot D}{\nu_{e-x}} = \frac{2 \times 0.08}{1.7894 \times 10^{-5}} = 8941.5 \quad Re_4 = \frac{V_4 \cdot D}{\nu_{e-x}} = \frac{2.8 \times 0.08}{1.7894 \times 10^{-5}} = 0.125 \times 10^5 \quad (10)$$

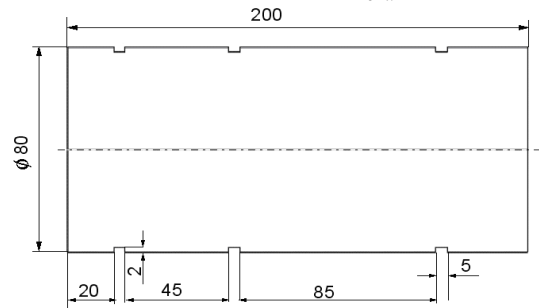


Fig. 1 Geometric model of observed area from the corrugated tube with threshold height $h_1=2$ mm.

The steps between two thresholds are different. For the first drawing (Fig 1) the height of the threshold is $h_1=2$ mm. The dimensionless ration between the height of

the threshold and the distance between the two thresholds calculated by equation (11) is:

$$Y_1 = \frac{P_1}{h_1} = \frac{0,045}{0,002} = 22,5; \quad Y_2 = \frac{P_2}{h_2} = \frac{0,085}{0,002} = 42,5 \quad (11)$$

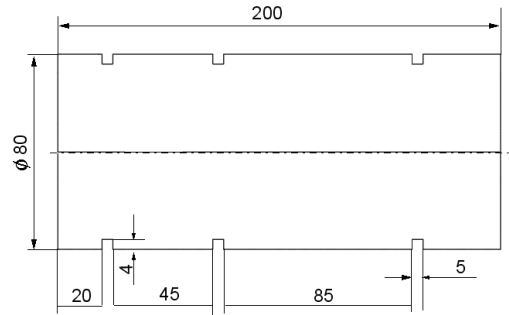


Fig. 2 Geometric model of observed area from the corrugated tube with threshold height $h_2=4$ mm

On (Fig.2) the height of the threshold is $h_2=4$ mm. The distance between the thresholds is different. The dimensionless

ratio between the height of the threshold and the step P – equation (12) is:

$$Y_3 = \frac{P_1}{h_1} = \frac{0.045}{0.004} = 11.25 ; Y_4 = \frac{P_2}{h_2} = \frac{0.085}{0.004} = 21.25 \quad (12)$$

3. Results and Discussions

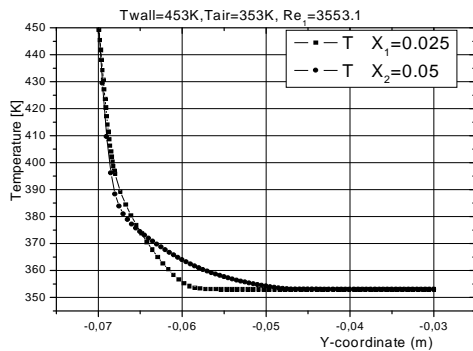


Fig.3 Temperature gradient in cross-section in the center for $Re_1=3353.1$ at two different thresholds X_1 and X_2

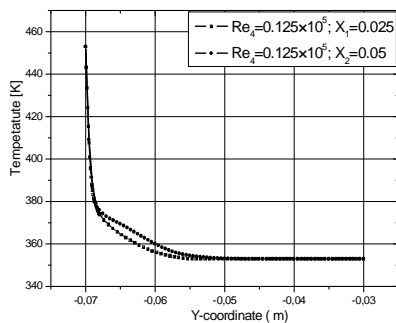


Fig. 4. Comparison of the temperature gradient in cross-section at $Re_4=0.125 \times 10^5$ at two different thresholds X_1 and X_2

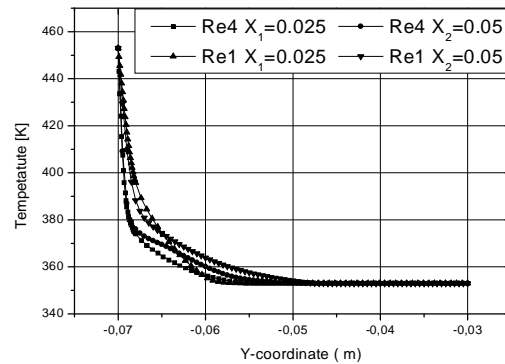


Fig. 5 Temperature gradient at the two heights of the threshold X_1 and X_2 for $Re_1=3353.1$ and $Re_4=0.125 \times 10^5$

The change in the flow character near the wall reflects in the distribution of the temperature and velocity towards the flow direction and perpendicular to the flow. The temperature profile change is most sensitive at the higher threshold ($X_2=0.05$) at the same Reynolds number.

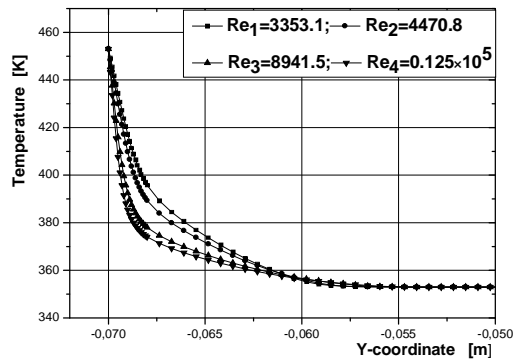


Fig.6. Influence of the Reynolds number on the temperature distribution at cross direction at X_1 .

On Figure 6 we can follow the influence of the Reynolds criteria on the temperature distribution at geometric model with relative height of the threshold – $X_1=0.025$. By increasing the value of Re the temperature profile is changed as it nears

the wall. The temperature profile at Re_4 is nearest to the wall, which means that at high Re values there will be the best heat transfer and the heat transfer surface will be used in the most effective way.

The observation of the location and the size of the circulation zone give opportunity for optimization of the shape and geometrical parameters of the threshold. After modulation and analysis of the circulation zone we can estimate the best solution for maximal effective heat transfer, which is the final goal of the numerical modulation. Every observation is performed after testing of the calculating mesh for adequacy and after proving the independence of the solutions from the thickness of the calculating mesh.

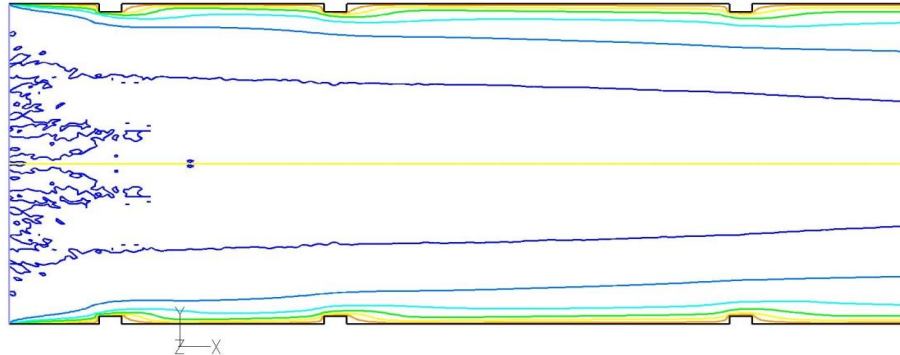
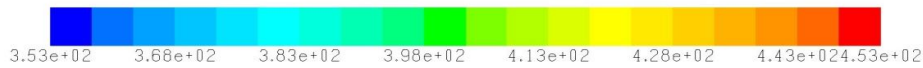


Fig.7 Constant temperature lines – isotherms, $X_1=0.025$ and $Re_1=3353.1$

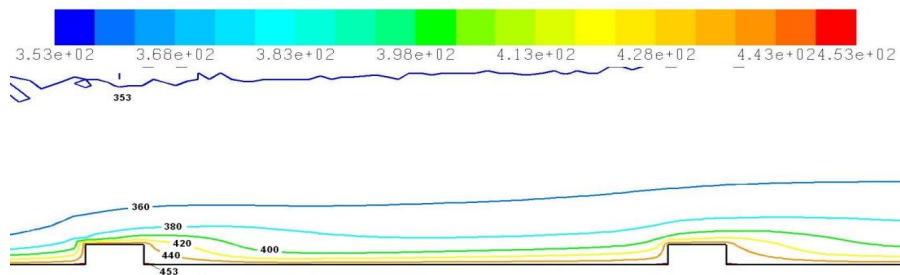


Fig.8 Constant temperature lines - isotherms, $X_1=0.025$ and $Re_1=3353.1$

Lines with constant temperature – isotherms have been calculated and drawn. The visualization of the isotherms near the flowed wall is of great interest regarding the intensification. The isotherms are drawn for equal temperature intervals – by 20 degrees. The most intensive heat transfer we have near the wall, not in the centre of the flow that is why it is important to show the temperature distribution exactly at this place. After comparison of the isotherms (Fig. 8 and Fig. 9) at the two heights of the thresholds we can make a conclusion for the

temperature gradient alteration. We can see that at the higher threshold the higher temperature isotherms are further from the wall. The prove for that statement is the visible difference in the temperature profiles near the wall (Fig. 11 and Fig. 12) at the two heights of the threshold and at same Reynolds number. This means that at higher threshold there is better heat transfer. The increase of the threshold dimension can not be done infinitely and there is a maximal value, up to which it can be increased.

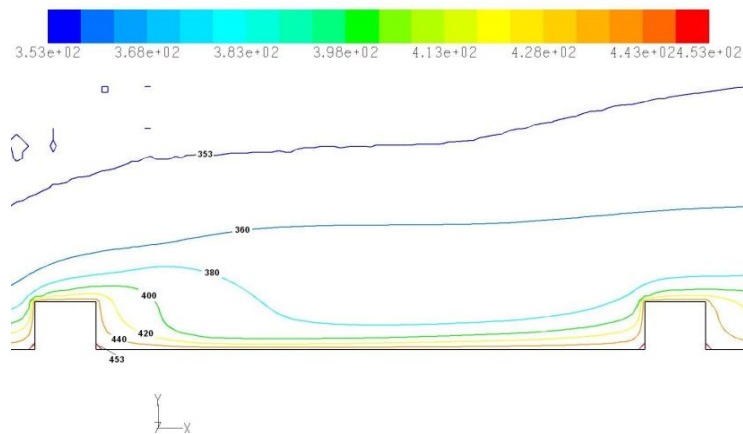


Fig. 9 Constant temperature lines - isotherms, $X_2=0.05$ and $Re_1=3353.1$

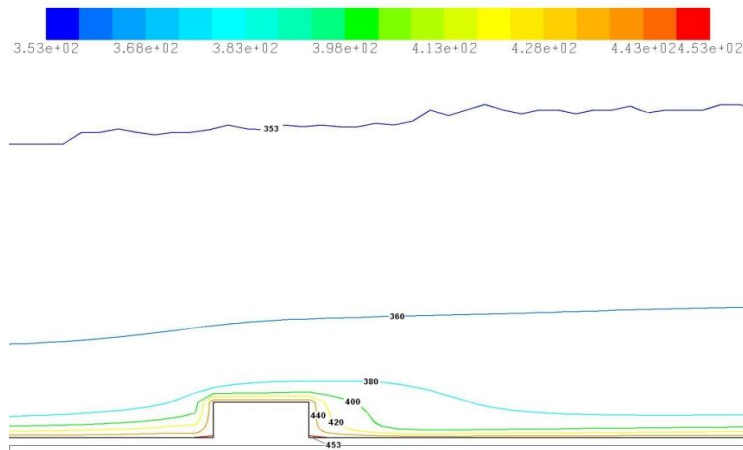


Fig.10 Constant temperature lines – isotherms, $X_1=0.025$ and $Re_4=0.125 \times 10^5$

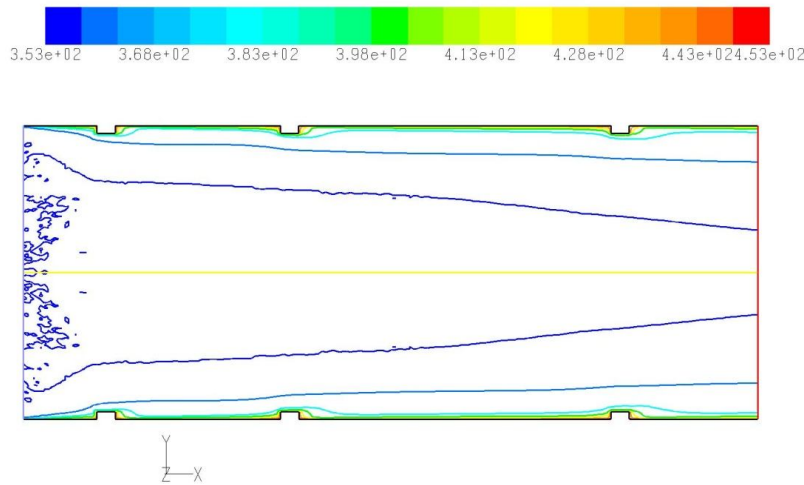


Fig. 11 Constant temperature lines – isotherms, $X_1=0.025$ and $Re_4=0.125 \times 10^5$

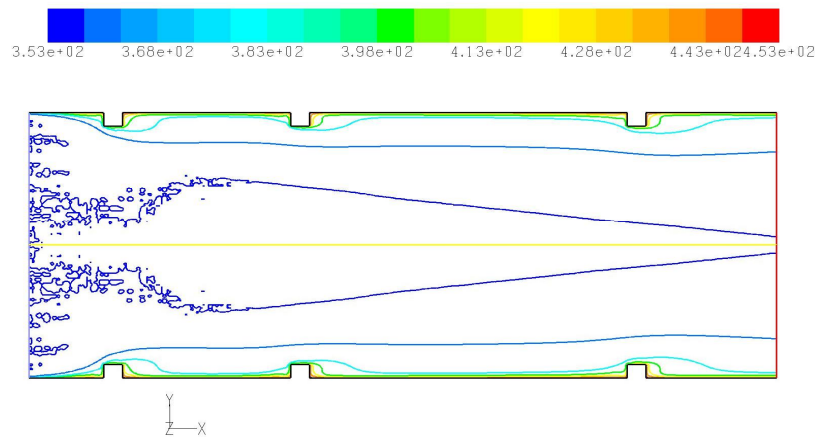


Fig. 12 Constant temperature lines – isotherms, $X_2=0.05$ and $Re_4=0.125 \times 10^5$

We can see on Figures 7, 11 and 12 the simultaneous impact of the higher threshold as well as of the higher Reynolds number. The correct choice of these two significant factors defines the good heat transfer between the heated surface and the cool fluid. At the exit on Fig. 12 there is the smallest cold sector, which means that the best heat transfer will be achieved if the height of the threshold is 4mm and $Re_4=0.125 \times 10^5$.

By comparison of the shape of the temperature profiles we can estimate the

influence of the corrugation and the velocity of the fluid on the temperature distribution in Y direction. At the highest values of the Reynolds number (Re_4) we have the highest value of the temperature of the heated fluid (air) at the outlet in perpendicular to the flow direction. We achieve better heat transfer at higher values of Reynolds number. If we combine enough high threshold and velocity of the flowing fluid at the outlet we can achieve the least cold zone. That is the important role of the calculating hydrodynamics and

the methods for modulation of such processes – because these modern calculation tools help making the right

choice for the best solution amongst the many variants of the given problem.

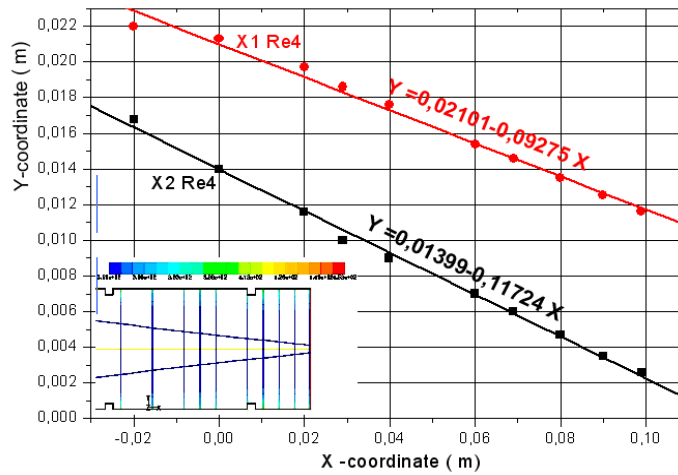


Fig.13 Influence of the threshold height on the temperature distribution

We can see on Fig. 13. the lines with the equations, which describe them for the size of the zone with temperature 353K. At the high threshold (X_2) at the outlet the section with temperature 353K is 0.0026m and at the lower threshold (X_1) it is 0.012m. We have mathematically described the dimensions of the zones with temperature 353K. The cold zone at the higher threshold is smaller, which means there is a better mixing and turbulization of the flow.

4. The higher the threshold – the better the heat transfer.
5. There is a better heat transfer at higher Reynolds number values.
6. If we combine high enough threshold and velocity of the fluid at the outlet, we achieve the smallest cold zone.
7. This research can be used for finding optimal values of the Reynolds number regarding the conditions for heat transfer.

4. Conclusion

On the base of the result, we can make the following conclusions:

1. The uneven step of the baffles leads to better picture of the wall flowing.
2. By increasing the criteria of Re we reduce the size of the non-flowing zone after the baffles, which leads to increasing the heat transfer.
3. The increasing of the temperature under the influence of the baffles is highly expressed in the direction of the flow.

5. References

- [1]. KOSTOV P., K. ATANASOV, N. KRASTEV, D. ANGELOVA. „Universal velocity profiles of twisted injected jet“, Scientific works tome LX “food science, technology and processes – 2013“ 18-19 October 2013, Plovdiv, pp.1531-1535. (in bulgarian)
- [2]. KOSTOV P, KRASTEV N, ANGELOVA D, Observation of injected radial jet at isothermal conditions – National Conference with international participation “Machine science”- 2012 – Sliven. Heat Technology 3, Year 3, Book 1 ISSN 1314-2550 pp. 8-11. (in bulgarian)

- [3]. KOSTOV P., KRASSTEV N., ANGELOVA D., DIMITROV I. „Estimation of temperature fields from flat-flame burner”, XVII scientific conference with international participation EMF 2012. pp. 86-90 http://www.tu-sofia.bg/faculties/emf/confer/documents/tom_1.pdf (in bulgarian)
- [4]. BERGLES, A. E. ExHFT for fourth generation heat transfer technology, *Exp. Thermal Fluid Sci.*, Vol. 26, Nos. 2-4, pp. 335-344, (2002).
- [5]. BERGLES, A. E. ExHFT for fourth generation heat transfer technology, *Exp. Thermal Fluid Sci.*, Vol. 26, Nos. 2-4, pp. 335-344, (2002).
- [6]. CATCHPOLE, J.P., DREW, B.C.E., Evaluation of some shaped tubes for steam condensers, *Steam Turbine Condenser, Report of a Meeting at NEL, Glasgow, UK*, pp. 68-75, (1974).
- [7]. MANGLIK, R.M., BERGELS, A. E, Enhanced Heat transfer in the New Millenium: A Review of the 2001 Literature, *Thermal Fluids and Thermal Processing Laboratory, Laboratory report № TFTPPL-EB01, University of Cincinnati, OH*, (2002).
- [8]. V. ZIMPAROV, Enhancement of heat transfer by a combination of a single – start spirally corrugated tubes with a twisted tape, *Experimental thermal and Fluid Science* 25 (2002) 535-546.
- [9]. V. ZIMPAROV, Prediction of friction factors and heat transfer coefficients for turbulent flow in corrugated tubes combined with twisted tape inserts. Part 2: heat transfer coefficients, *International Journal of heat and Mass Transfer* 47 (2004) 385-393.
- [10]. Ö. AĞRA, H. DEMIR, Numerical investigation of heat transfer and pressure drop in enhanced tubes, *International Communications in Heat and Mass Transfer* 38 (2011) 1384-1391.